



Research on coupling theory and its experiments between torque turbulence and bearing load of multi-support-rotor systems

Xinyu Pang and Zhaojian Yang

College of Mechanical Engineering, Taiyuan University of Technology, Taiyuan, Shanxi, China

ABSTRACT

The bearing load (BL) governs the stability of axes set in the multi-support-rotor systems (MSRS). The torque turbulence (TT) would change BL, which could cause instability of axes set. In order to discern the torque turbulence, the theoretical analysis about the TT effecting on the BL had been done, as well as the coupled model about TT and BL had been established, and the experimental study was presented in the paper. The two-directions bearing load sensor was introduced and its dynamic characteristic was analyzed as well according to its measuring principle and structure feature. Indirectly measuring the load of bearing bracket in radial and axle direction, the sliding bearing load could be acquired. An eight-support rotor test rig which is a MSRS with sensor was established, and its dynamics character was analyzed. The coupled model about TT and BL was set up. Finally, the experiment about BL in different support positions with two typical TT had been done. With the experimental results, it was manifested that the bearing load sensor has the characteristics of highly sensitivity, and the bearing load value could be monitored online when the TT exerted on the rotor system. The coupled model is verified, which provided the theoretical foundation and test data for the torque turbulence recognition.

Keywords: Multi-support-rotor system, bearing load, torque turbulence, sensor, dynamic characteristic

INTRODUCTION

MSRS is the key component for the large-scale rotation equipments such as the steam turbine and the compressor, etc. For calculating the bearing load of MSRS, the method of transmission matrix has been applied in a long period [1], and the result is just a reference function for installing the set of axes. There is little effect on the elevation adjustment and the failure predication. Besides the support position movement, the bearing load is affected by the moment of torque turbulence which is caused due to the load change in electrical wire netting, the defect in steamer blade and so on. Then the rotational speed of the rotor is disturbed. The stability of the system is finally destroyed [2]. Therefore, testing the bearing load with the most effective examining instrument directly and catching the feedback information real-time are very great significance for keeping the set stability and avoiding the pernicious accident.

Generally, there are four kinds of methods which would be adopted in discerning the load of utility-type unit[3]. 1) Dynamometry. It can be described that a dynamometric device is installed between the bearing and bearing bracket, and then the load could be measured directly. 2) Deflection method. It can be explained that the static displacement between the axle journal and the bearing is tested, and then the load can be calculated by analyzing the characteristic of oil layer. 3) Elevation method. It can be interpreted that the dynamic elevation is examined, and then the bearing load is obtained by calculating the value of the elevation. 4) Pressure method. The bearing load is discerned by measuring pressure of the oil film. So, the dynamometry is the best way among them. Nevertheless, there is a little difficulty in installing the sensor because of the structure limitation between the bearing and its bracket. The brackets are usually fixed on the base with the bolts when rotor systems work. In this paper, the two-directions bearing load sensor was introduced and fixed between the bracket and its base. The force acted on the sensor by the

bearing bracket can reflect on the bearing load. The MSRS kinetic model and the TT-BL coupling model are established, and the structure of the bearing load sensor was described. Meanwhile, the dynamic characteristic of the sensor was analyzed and the dynamics of the support structure with sensor is analyzed. Furthermore, some experiments about BL in the different support positions were done with the mentioned sensor.

I. BEARING LOAD-SENSOR

A. Principal and structure of sensor

The bearing load was realized by indirect measurement. The measuring principle is resistance strain. The so-called indirect measurement is that the bearing load transfers to the sensor by the bearing housing. The load-sensor outputs different voltage signals which are converted from resistance values of the strain gauge through the full bridge circuit. The sensor is made of hard aluminum alloy material, on the one hand because of its good elasticity, on the other hand, because of its high strength. The structure of the load-sensor is shown in Fig.1.

When the load body of the sensor was bearing the horizontal and vertical loads of bearing bracket, the beam would deform greatly. In the neutral layer of the beam, the shear stress and strain are maximum. However, the shear stress was not measured easily and it could only produce the two perpendicular main stress and angle of 45 degree to the beam central axis, which caused the maximum tensile stress and compressive stress. Thus, four blind holes were processed respectively in the horizontal and vertical beam segments. The two strain gauges were pasted along two directions perpendicular each other which are angle of 45 degree to the central axis beam, where the bending moment was zero in the bottom of the hole. Strain gauges R1, R2, R3, R4 were pasted onto the bottom of blind hole on the left and right horizontal segments of the beam, R5, R6, R7, R8 were pasted onto the bottom of blind hole on the vertical segments of the beam. R1, R2, R3, R4 formed a full-bridge circuit, as shown in Fig.2. (a), to measure the bearing loads of Y direction. R5, R6, R7, R8 generated a full-bridge circuit, as shown in Fig.2. (b), to measure the bearing loads of X direction.

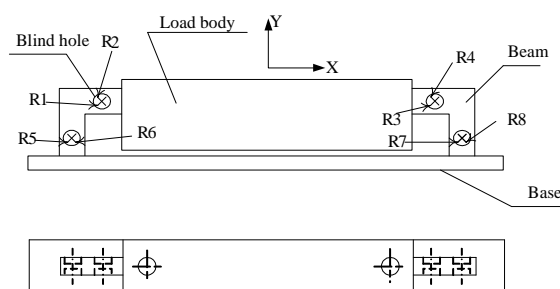


Fig.1: The structure of bearing-load sensor

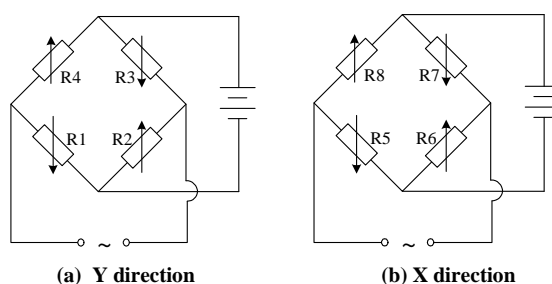


Fig.2: Full-bridge circuit

B. Analyze the dynamic characteristics

The dynamic characteristics were analyzed using both transient response and frequency response from the time domain and frequency domain [4]. Commonly the response characteristics are obtained through step function in the time domain and through sine function in frequency domain. Dynamic performance indexes are mainly natural frequency and damping ratio. Natural frequency of the sensor is determined mainly by the structure parameters. The higher the ω_n value, the faster the response of the sensor. With the "virtual experiment system on mechanical control engineering", the dynamic characteristics were analyzed. The virtual experimental system was developed on the basis of the mechanical control theory, for time domain response, frequency domain response and stability analysis of typical part.

According to structural parameters of the sensors, the vibration mass (m), stiffness (K) and equivalent damping coefficient (C_e) were calculated respectively, $m=1.68\text{kg}$, $K = 4.14 \times 10^7 \text{ N} \cdot \text{m}^{-1}$, $C_e \approx 10000$. Substituting these values into the virtual experimental system, frequency response curve could be obtained under the step input shown in Fig.3.

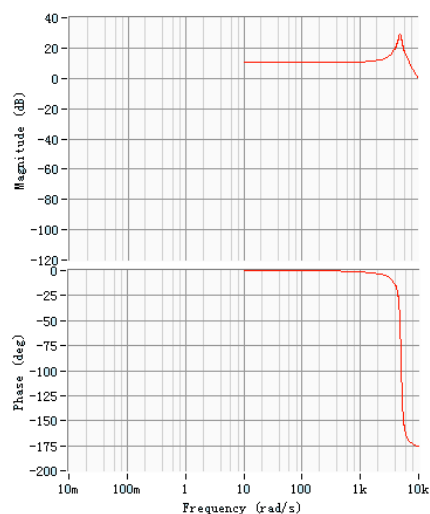


Fig.3: Frequency response curve

To reflect the dynamic performance of the sensor to certain extent, the signal of linear loading process was sampled by the DASP data collection instrument in this paper. The loading speed of X direction is 0.1mm / s, and that of Y direction is 0.08 mm/s. The output curves were shown in Fig.4. The Fig.4 reflected the sensor can track the dynamic signal quickly and accurately, and the dynamic characteristics were good.

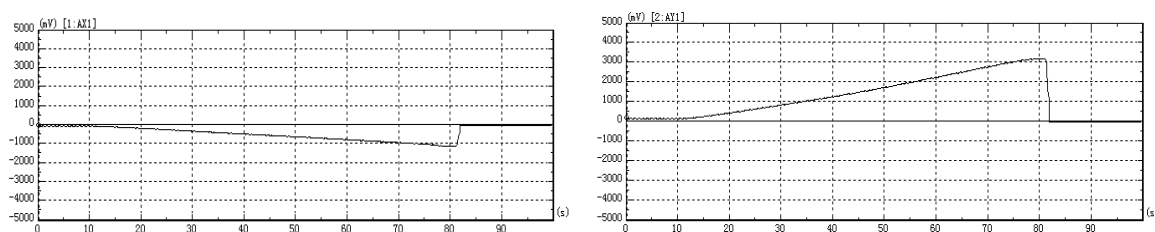


Fig.4: X and Y direction sampled curves

C. Dynamic analysis of the support structure with sensor

The finite element model of the support structure with the sensor was shown in Fig.5. Structural element type was Solid185; material property was bearing material-Q235, linear and isotropic, so its elastic modulus $E = 210\text{GPa}$, Poisson's ratio $\mu = 0.3$, density $\rho = 7800\text{g/cm}^3$; the sensor material is the hard aluminum alloy, so the definition of the elastic modulus $E = 70\text{GPa}$, Poisson's ratio $\mu = 0.3$, density $\rho = 2700\text{g/cm}^3$.

After the geometric model had been created, the model was meshed using free mesh [4]. Analysis type was the Modal. The mode extraction method was the Block Lanczos method. Modal extraction number was 5. Extracted mode frequency range was the default value. The number of modal extended was 5. Modal analysis of the loading only included displacement constraints. All the nodes of the bottom of sensor were selected as constraint point, and its constraint type was "All DOF". The result to illustrate natural frequencies of the 1st~5th order from Post-Processor (POST1) can be seen in Tab 1.

Tab 1. The 1st~5th order natural frequencies of the support structure with the sensor

Step	1	2	3	4	5
Natural frequencies (Hz)	205.1	829.21	917.75	964.15	1391.6

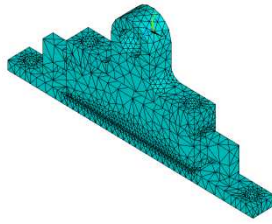


Fig. 5: The finite element model of the support structure with the sensor

II. THE DYNAMICS ANALYSIS ON THE MSRS

A. The MSRS test rig

The structure of the test rig was shown in Fig. 6. 3D model was shown in Fig.7. The test stand was a simulation test stand of the Turbo. The axes was formed by the four axis connected by rigid coupling. And each axis was installed with two 50kg round iron plates for simulating the actual quality of the rotor accessory such as the impeller. The axes was driven by the motor, and its rotation speed could be adjusted by frequency converter up to 3000r/min. Between each bearing housing and the base, 8 sensors were mounted on each support point. The end of the shaft was the magnetic brake that can be used to change the torque. In addition, vibration sensors, torque sensors and data collection instrument were contributed to form a complete test system, used for fault identification and diagnosis [5].



Fig. 6: The structure of the test stand

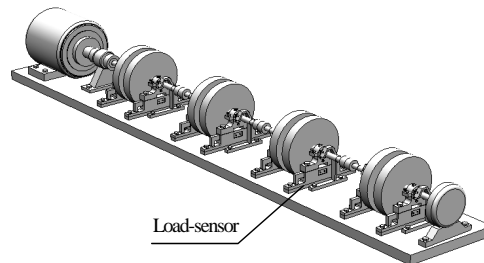


Fig.7 3D model of the test stand

B. The dynamics model for MSRS

The MSRS is an elastic system which has the feature of the mass continuous distribution [6]. In order to analyze the dynamics character, the succinct and reasonable mechanics model must be established. The mass and the rotation inertia of the shaft were distributed to two ends, which formed the integrated-rigid-disc. The axes itself was simplified to the uniform-section elastic shaft without any mass in Fig.8. The positions at the bearing support were called exterior node, and else were called interior node.

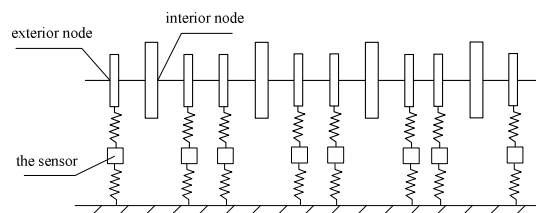


Fig.8: The mechanics model for MSRS

So far as the MSRS be concerned, there are four kinds of forces, the spring force, the damping force, intersectional spring force and intersectional damping force, because of the kinetic lubrication bearing existing at the external nodes. The force at the external nodes, F , consisted of the inertial force, the spring force, the external damping force and the out-of-balance excitation force. However, there are only two kinds of force, the inertial force and the excitation force, at the interior node [7]. In the paper, the axes and the bearing were regarded as one external node. For analyzing mainly the structure formed by the sensor combined with bearing support, and the external damping force and the intersectional stiffness excitation force were not taken into account. Assuming the base is rigid and the bearing bracket is regarded as elastic support, which was equivalent to an elastic body when the sensor was installed between the node and the base. The mass participating in vibration included bearing bracket mass and the sensor mass. The Fig. 9 shows the structural mechanics model on the XY datum.

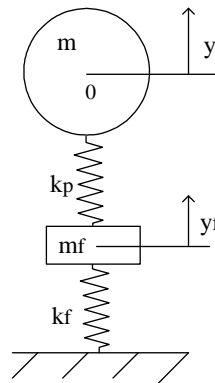


Fig. 9: The structural mechanics model when the bearing load sensor was installed

Where, y is the distance-the node center deviated from its static equilibrium position; y_f is the distance-the sensor deviated from its equilibrium position; k_p is the isotropic spring stiffness coefficient of the simplified bearing; k_f is the isotropic spring stiffness coefficient of the simplified sensor; m is the external node mass participating in vibration which includes the integrated-rigid-disc mass, the bearing mass and the bearing bracket mass; m_f is the sensor mass participating in vibration. So the mechanics equations at the external node could be described as following:

$$\begin{cases} F = m\ddot{y} + k_p (y - y_f) \\ k_p (y - y_f) = m_f \ddot{y}_f + k_f y_f \end{cases} \quad (1)$$

C. The axes dynamics equation

The MSRS is a multi-degree of freedom system. Besides the oil film coupled force, there were the coupled effects among the each bearing support force. Supposed the amount of support position as n , and the coupled effect was taken into account in the MSRS, then dynamics equations (2) as following could be established based on the formula(1).

$$\begin{cases} [M]\{\ddot{Y}\} + [K_p]\{Y - Y_f\} = [M]e \sin(\Omega t + \beta_i) + \{F\} \\ [M_f]\ddot{Y}_f + [K_f]Y_f = [K_p]\{Y - Y_f\} \\ \{F\} = [Q]\{\Delta F\} \end{cases} \quad (2)$$

where: $[M] = [m_1, m_2, \dots, m_n]$ is the concentrated mass at different support points. $[M_f] = [m_{f1}, m_{f2}, \dots, m_{fn}]$ is the participation vibration mass at different support points. $[K_p] = [k_{p1}, k_{p2}, \dots, k_{pn}]$ is the stiffness of the each sliding bearing. $[K_f] = [k_{f1}, k_{f2}, \dots, k_{fn}]$ is the stiffness of support. $\{Y\} = \{y_1, y_2, \dots, y_n\}$ is the vibration displacement of the each support point along vertical direction. $\{Y_f\} = \{y_{f1}, y_{f2}, \dots, y_{fn}\}$ is the vibration displacement of the each participation mass at the support point. $\{F\} = \{f_1, f_2, \dots, f_n\}$ is the support coupled force at the different support point. $\{\Delta F\} = \{\Delta f_1, \Delta f_2, \dots, \Delta f_n\}$ is the value of the bearing load fluctuation at different support point. $\{Q\}$ is the sensitive coefficient of BL [8].

D. The BL model under the condition of TT

When the position of bearing is defined, the dynamic load of bearing is related to the rotor revolution. The faster of revolution was, then the larger of eccentricity of the axle journal mounted by the bearing was, and the load along Y direction became less. Obviously, the rotor rotation speed was changed directly by TT. Then the dynamic load of bearing was interfered with TT. For the single-span rotor structure, the rotation speed of the axes became low transient under the condition of TT. Additional load ΔF was also generated. The mapping relationship between the value of the BL fluctuation and the torque was described as following:

$$\Delta F = \sum_{j=1}^m \alpha_j K(T_j, T) \quad (3)$$

Where, α_j is the torque factor. T is the external torque. $K(T_j, T)$ is the radial base kernel function.

Supposed $X = \{\Delta F_i\}_{i=1}^m$, then $D = \{X_i, T_i\}_{i=1}^m$ represents a set of training data. Supposing the parameter vector for discernment as $X_s = [\alpha_1]$, and then T could be defined according to the equation (4).

$$\begin{cases} J\ddot{\theta}_y + k_1\left(\frac{L}{2}\right)^2 \theta_y - k_2\left(\frac{L}{2}\right)^2 \theta_y + \alpha_1 \cdot T\left(\frac{L}{2} + L_T\right) = 0 \\ \theta_y \approx y_1 - y_2 \\ F_{y1} = k_1 y_1 \\ F_{y2} = k_2 y_2 \end{cases} \quad (4)$$

Where, θ_y is tilt angle in the y direction; k_1 and k_2 are the stiffness at its own support point. y_1 and y_2 are the respective vertical displacement at two support points. L is the span distance between two support points. L_T is the distance from the TT position to support point. F_{y1} and F_{y2} are the respective BL at the support point. Then the objective function could be defined as follows:

$$J(f) = C \sum_{i=1}^m L(T, T_{si}) + \frac{1}{2} \langle f, f \rangle = C \sum_{i=1}^m L(f(T), T_{si}) + \frac{1}{2} \langle f, f \rangle$$

Where, $L(f(T), T_{si})$ is the loss function. T_s is the measured torque, C is the penalty function. $J(f)$ is the minimum for identification object.

\mathcal{E} was adopted as insensitivity loss function in SVM standard. Then the loss function can be described as follows:

$$L(f(T), T_{si}) = |f(T) - T_s|_{\mathcal{E}} = \begin{cases} 0 & |f(T) - T_s| < \mathcal{E} \\ \mathcal{E} & \text{others} \end{cases}$$

Three steps should be taken for finishing the computational process above mentioned [9][10]. The first is constructing the training sample for $D = \{X_i, T_i\}_{i=1}^m$. The second is selecting the model which supports the vector machine. The regression algorithm supporting vector machine model was determined by kernel function, loss function and capacity control. The radial base kernel function is adopted because of its stronger ability of generalization. The last step is obtaining the optimization solution. Then the BL model under the condition of TT with the number of support points of n in MSRS was described as follows:

$$\{\Delta F_i\} = \left\{ \sum_{i=1}^n \sum_{j=1}^m \alpha_{ij} K(T_{ij}, T_i) \right\} \quad (5)$$

III. THE EXPERIMENT OF BL UNDER OF THE CONDITION OF TT

A. The experiment process

In order to analyze the relationship between TT and BL, the experimental solution was designed as follows: two different kinds of TT were exerted respectively on MSRS when the rotor ran at acceleration phase, constant-speed phase and deceleration phase. Then the curves of bearing load could be acquired. The infinite variable speed of the rotor was realized by the motor which was controlled by the frequency converter. The maximum rotation speed of rotor was 500r/min. The sample frequency is 512Hz. The experiment parameters were shown in Tab.2.

Tab.2 The run status and data of MSRS

Run status	Acceleration phase	Constant-speed phase	Deceleration phase
Duration(s)	0-180	181-380	381-560
The moment of impact torque working (s)	20	90,130	160
The moment of linear torque working (s)	20~30	100~130	160~170

Under the condition listed in Table. 2, the impact torque curve and linear torque curve of the rotor were shown respectively in Fig.10 and Fig. 11.

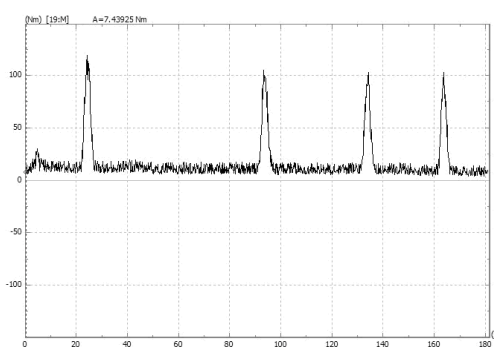


Fig.10: The impact torque

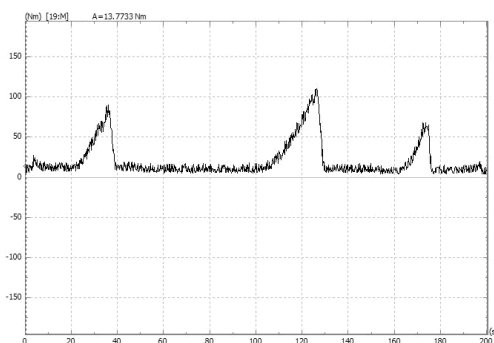


Fig.11: The linear torque

B. Experiment result

The results of the BL along X direction and Y direction were shown in Fig. 12, which were the system response under the condition of impact torque turbulence.

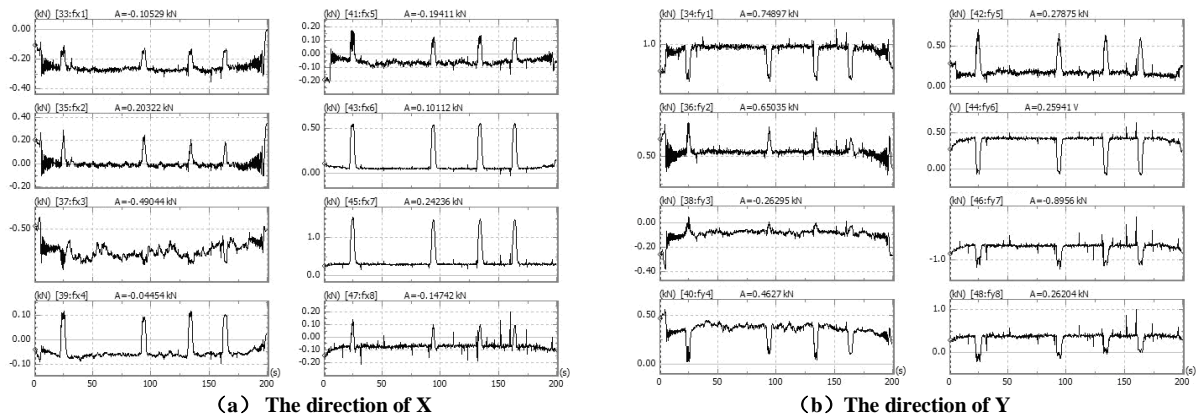


Fig.12: The variation torque contours of the rotor under the condition of impact torque turbulence exerted

The results of the BL along X direction and Y direction were shown in Fig. 13, which were the system response under the condition of linear torque turbulence.

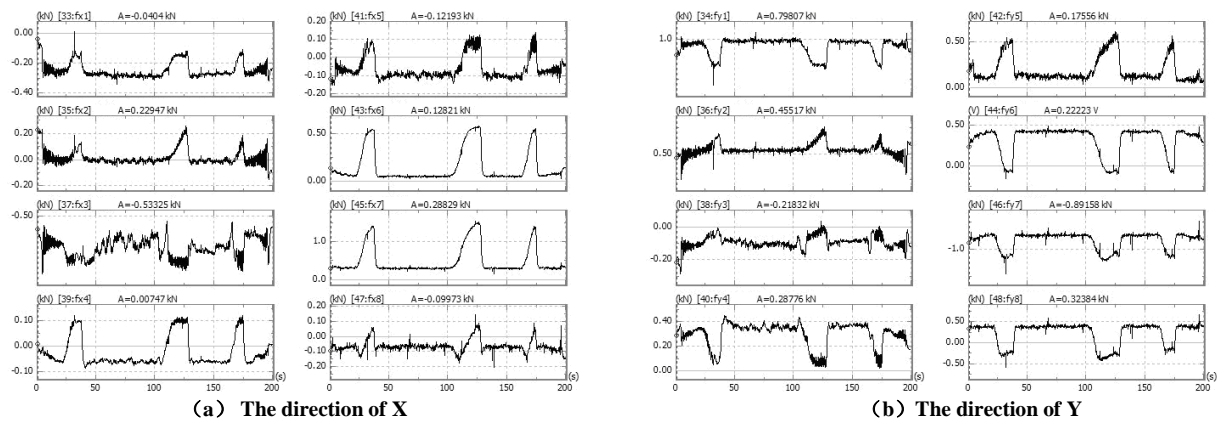


Fig.13: The variation torque contours of the rotor under the condition of linear torque turbulence exerted

The TT must lead to the reducing of rotational speed of the rotor and the decline of eccentric rate. It can be seen in Fig. 12 and Fig. 13. The variation tendency of the each support load was examined in the experiment when the rotor worked in the turbulence torque exerted. Intervened torque turbulence, the variation contours of the bearing load and the torque was almost in the same tendency. The bearing load was extremely greater than it without torque turbulence exerted in the same rotation speed. Torque turbulence being away from the nearest support point, the variation of bearing load was greater than that of other position.

CONCLUSION

a) The bearing load sensor was installed between the bearing bracket and base. It could not change the structure of the bearing. So it would not have influence to the bearing. The sensor has the better dynamic characteristic and the higher sensitive. The critical speed of revolution could be derived by analyzing its dynamics property; as a result, the operating rotation speed could be obtained.

b) It was manifested in experiment that the bearing loading in each support point was generating the remarkable variation when the torque turbulence exerted on the axes set. Its amplitude of variation was even higher than the load caused by changing the position of bearing. It is sure that measuring BL after TT exerted is greatly effective in real-time testing BL of MSRS.

Acknowledgements

This work was supported by National Natural Science Foundation of China (NSFC) (Grants: 51075292).

REFERENCES

[1] L.X. Xu. *Dynamic Design of High-Speed Rotary Shaft*, 1st Edition, National Defense Industry Press, Beijing, 1994; 103-108

-
- [2]H.E. Sun. Flexural Vibration Performance of Multiple-disk Rotor Systems of Slender Shafts Based on Torsional Excitation, Taiyuan University of Technology, Taiyuan, **2010**;1-18.
- [3]Y. Chen; X.Y. YUAN ; Q.J. Meng. *Northwest China Electric Power*, **2001**,5: 29-42.
- [4]X.Y. Pang; Z.J. Yang; Q.L. Liang; H.E. Sun. *Journal of Taiyuan University of Technology*, **2009**, 40 (5): 461~464 [5]X.Y. Pang; Z.J. Yang; Q.L. Liang; H.E. Sun and H.F. Mei. *Turbine Technology*, **2010**, 52 (5) : pp. 332-335
- [6]Z.J. Yang ; Y.B. Xie. *China Mechanical Engineering*, **1997**, 4 (8):89~91.
- [7]B.C. Wen: *Advanced Rotor Dynamics*, 1st Edition, Machinery Industry Press, Beijing, **2000**;89-103
- [8]Z.J. Yang ; Z.J. Peng. *KSME International Journal*, **2004**, 18(6) : 946~954.
- [9]H.R. Wang ; Q. Liu. *Journal of Huaqiao University(Natural Science)*, **2010**, 31(2) : 132-135.
- [10]F. Ning; D.M. Ji ; X.P. Yao. *Journal of Chinese Society of Power Engineering*, **2010**, 30 (3) : 166-169.